

Suppression of interfering ions by using ionic liquid and micelle moieties in spectrofluorimetric analysis of manganese

Özlem ÖTER^{1,*}, Müge AYDIN², Kadriye ERTEKİN¹

¹Department of Chemistry, Faculty of Science, Dokuz Eylül University, Buca, İzmir, Turkey

²The Graduate School of Natural and Applied Sciences, Dokuz Eylül University, Buca, İzmir, Turkey

Received: 17.06.2015

Accepted/Published Online: 10.11.2015

Final Version: 17.05.2016

Abstract: Eosin-Y exhibits high affinity and emission based spectral response to most of the major ions in water samples. In the present study we performed selective spectrofluorimetric analysis of manganese with eosin-Y in the presence of potential interferents. We employed green chemistry reagents, ionic liquids (ILs) and two different micelles, to suppress the effect of conventional cations and anions on the response of eosin-Y. The experimental data revealed that different test moieties caused enhanced analytical response to Mn²⁺. The highest analytical signal of eosin-Y was obtained in the presence of Triton X-100 at a concentration of 2.0×10^{-3} mol L⁻¹. Presence of the green chemistry reagents ILs enhanced the limit of quantification for Mn²⁺ 10-fold with respect to the IL-free moieties. The interfering effects of the metal ions of Ca²⁺, Cu²⁺, Hg⁺, Hg²⁺, As⁵⁺, Li⁺, Al³⁺, Cr³⁺, Co²⁺, Ni²⁺, and the anionic groups were completely suppressed in the presence of the ILs and micelles. Additionally, the tolerance limit of Na⁺ and Zn²⁺ ions increased 6-fold in the presence of IL and sodium dodecyl sulfate. The presented method did not use any harmful conventional solvents and was employed successfully for the detection of Mn²⁺ ions in real water samples.

Key words: Ionic liquids, micelle, eosin-Y, Mn²⁺

1. Introduction

Manganese plays a significant role in the human body as a component of enzymes and in plants for photosynthetic evolution of oxygen.^{1,2} On the other hand, prolonged exposure to even low levels of manganese has toxic effects and can cause diseases such as Parkinsonian disturbances.³ There are several analytical techniques for determination of Mn²⁺. Flame and electrothermal atomic absorption spectrometry (FAAS, ETAAS),^{4,5} inductively coupled plasma techniques (ICP-OES, ICP-MS),⁶ neutron activation analysis,⁷ X-ray fluorescence,⁸ voltammetry,⁹ and molecular absorption spectrophotometry¹⁰ are typical determination methods. Despite their satisfactory limits of detection (LOD), ICP and AAS are costly and destructive methods. Therefore, the spectrofluorimetric method is a good alternative because of its relative simplicity, low cost, high sensitivity, real-time detection ability, and competing LOD values with atomic spectroscopic techniques. However, only a few fluorescent sensors for Mn²⁺ have been reported to date. A novel recognition method for Mn²⁺ ions with CdTe quantum dots was developed by Shulong et al.¹¹ Liang and Canary used a 1,2 bis-(o-aminophenoxy)ethane-N,N,N,N-tetraacetic acid (bapta) based fluorescent probe for detection of Mn²⁺.¹² Mao et al. employed 1,2-bis-(2-pyren-1-ylmethylamino-ethoxy) ethane on the surface of graphene nanosheets.¹³ A new approach based

*Correspondence: ozlem.oter@deu.edu.tr

Table 1. Comparison of the Mn²⁺ sensing properties of different dyes in different moieties.

Sensitive dye	Sensing medium	Dynamic working range	Detection limit	Selectivity	Ref.
1-Thioglycerol-capped CdTe quantum dots	Buffer solution at pH 11.0	10 nmol L ⁻¹ –5 mmol L ⁻¹	10 nmol L ⁻¹	Sensitive to pH and Cu ²⁺	11
Ligand 1 obtained by substitution of carboxylate groups of BAPTA with pyridines	In HEPES buffer at pH 7.2	-	-	Selective to Mn ²⁺ over Ca ²⁺ , transition metal ions, Ni ²⁺ and Cu ²⁺ quench the fluorescence, while Fe ²⁺ , Co ²⁺ , Zn ²⁺ , Cd ²⁺ , and Hg ²⁺ may interfere with Mn ²⁺ binding	12
Water soluble fluorescent copper nanoparticles	Aqueous solution	0.25–250 µM	1.6 µM	The removal of Fe ³⁺ and Pt ²⁺ was required to avoid the interference	13
(6E)-N-((E)-1,2-diphenyl-2-(pyridin-2-ylimino)ethylidene)pyridin-2-amine	In 1:1 (v/v) CH ₃ CN:H ₂ O solution at pH 4.2.	2 × 10 ⁻⁴ – 7.2 × 10 ⁻⁴ M	-	At 1.0 mM metal ions, K ⁺ , Co ²⁺ , Zn ²⁺ , Pb ²⁺ , and Ag ⁺ quench the fluorescence intensity (FI) of ligand to a small extent while Fe ²⁺ and Hg ²⁺ ions quenched considerably. Little enhancement in FI with metal ions of Na ⁺ , Mg ²⁺ , Ba ²⁺ , Ca ²⁺ , Ni ²⁺ , Cu ²⁺ , and Cd ²⁺ .	36
Mordant brown 33 (MB33)	Tween 20–pH 9.0 Thiel buffer–ethanol mixture	1.1–4.40 µg mL ⁻¹	0.046 µg mL ⁻¹	The determination of manganese was possible in presence of Li ⁺ , Na ⁺ , K ⁺ , NH ₄ ⁺ , Mg ²⁺ , Ba ²⁺ , Mn ²⁺ , Zn ²⁺ , Cd ²⁺ , SO ₄ ²⁻ , SO ₃ ²⁻ , NO ₃ ⁻ , Cl ⁻ , Br ⁻ , I ⁻ , CN ⁻ , and PO ₄ ³⁻ (≈ 100-fold excess), as well as Pb ²⁺ , Cr ³⁺ , Co ²⁺ , Ni ²⁺ , Ag ⁺ , Al ³⁺ , Mo ⁴⁺ , Ca ²⁺ , As ⁴⁺ (≈ 50-fold excess).	37
Toluidine blue	In water–organic media (the extraction of organic phase is necessary).	0.1–2.9 µg mL ⁻¹	-	The determination is interfered by Cr ⁶⁺ and Ca ²⁺ .	38
2-Hydroxyquinoline	-	-	Submicromolar concentration	Various metal ions considerably interferes so the separation and/or masking of these undesirable metal ions is advisable	39
2-Hydroxy-1-naphthaldehyde salicyloyl hydrazone with hydrogen peroxide	In a water–ethanol (5.5–4.5, v/v) medium at pH 10.90	0.0 to 50 ng mL ⁻¹	0.97 ng mL ⁻¹	Except EDTA no ion interferes at the same level of Mn ²⁺	40
Eosin-Y	Surfactant containing acetic acid/acetate/EtOH solutions at pH 5.0	0.001– 3.0 mg L ⁻¹	2.5 × 10 ⁻⁴ mg L ⁻¹ (0.25 ng mL ⁻¹)	Interferent effects of Ca ²⁺ , Cu ²⁺ , Hg ⁺ , Hg ²⁺ , As ⁵⁺ , Li ⁺ , Al ³⁺ , Cr ³⁺ , Co ²⁺ , Ni ²⁺ , Na ⁺ , Cd ²⁺ , Zn ²⁺ , Mo ²⁺ , Pb ²⁺ , Mg ²⁺ , and Fe ³⁺ were significantly suppressed.	This work

on supramolecular metal displacement by fluorescence “off–on” mode was reported by Gruppi et al.¹⁴ However, some of these agents are subject to interference from other metal ions. Some commercial dyes are known to show fluorescence after interaction with Mn²⁺ but they lack selectivity for Mn²⁺ particularly, besides Ca²⁺

ions.¹⁵ Ca^{2+} , Mg^{2+} , Na^+ , and K^+ ions are important interferents due to their high abundance in physiological samples as well as in natural waters.¹⁶ Therefore, selectivity is an important requirement for the analysis of manganese ions and there is a need to develop new analytical procedures especially focusing on selectivity and sensitivity problems. Previous studies on the determination of Mn^{2+} ions are compared in detail in Table 1 in terms of the sensing dye, the analysis media, linear working range, detection limit, and selectivity.

In this work, we focused on selective determination of manganese by exploiting a general biological stain and a chelate maker, eosin-Y, in imidazolium-based ionic liquids (ILs) and in micelles. It had been previously reported that the addition of cationic and anionic surfactants or micelles to the sensing media increased the sensitivity and selectivity of the analytical method. When charged surfactants (e.g., sodium dodecyl sulfate (SDS)) were used, increased relative signal changes were reported.¹⁷ There are also some studies indicating that ILs may constitute a new class of surfactants with special properties resulting in considerable enhancements in analytical response.^{18,19} In recent years, it has also been shown that ILs supplied a stable and sensitive environment in some analytical applications.^{20–22} There are increasing numbers of studies on the preconcentration or selective extraction of metal ions using ILs.^{23–32} All these studies encouraged us to test some well-known ILs and surfactants as signal enhancers for the spectrofluorimetric analysis of manganese with eosin-Y for the first time. In this way, we suppressed the potential interferents and enhanced the sensitivity and selectivity of the method. LOD values extending to nanogram per liter were attained. Effects of pH and the interfering ions on spectral response were tested and evaluated. Recovery tests were successfully performed for real water samples.

2. Results and discussion

2.1. Spectral characterization of eosin-Y dye

Spectral characterization of eosin-Y was performed in solutions of S1–S6. Figure 1 shows the emission spectra of eosin-Y in the solutions. The dye exhibited broad emission bands ranging from 510 to 660 nm with emission maxima of 545–554 nm depending on the solution media. It should be remembered that the imidazolium-based ILs have nonnegligible absorption and intrinsic fluorescence in the visible region of the electromagnetic spectrum, which can affect the emission of eosin-Y. However, the absorption band of the utilized ILs did not cause a significant overlap with the excitation band of the eosin-Y. Therefore, we did not observe an IL-dependent decrease in the fluorescence intensity of eosin-Y up to 40% concentration of IL. However, at higher concentrations, a quenching of fluorescence intensity was observed. Thus, concentrations of the ILs in the solutions were kept between 2.14×10^{-2} and 2.61 M. The exploited ILs in the given concentration range also did not cause any spectral shift. However, in the case of micelle forms, the dye exhibited a red shift of 3 nm in the presence of SDS. TX-100 caused a moderately longer red shift of 9 nm and a slight decrease in fluorescence intensity (see Figure 1). This result is in accordance with the literature, which states that at surfactant concentrations at critical micelle concentration (CMC) and above, the solubilizing effect of the micelles begins to be important. Probably, the ion-association complexes are incorporated into the micelles and this causes some new changes in spectral responses of the indicator dye.^{33,34}

2.2. Response of eosin-Y to different cations/anions and selectivity studies

Response of eosin-Y to metal ions was investigated by exposure to 1.0 mg L^{-1} Ca^{2+} , Cu^{2+} , Hg_2^{2+} , Hg^{2+} , As^{5+} , Mo^{2+} , Li^+ , Pb^{2+} , Al^{3+} , Cr^{3+} , Na^+ , Mg^{2+} , Zn^{2+} , Cd^{2+} , Fe^{3+} , Co^{2+} , and Ni^{2+} in different

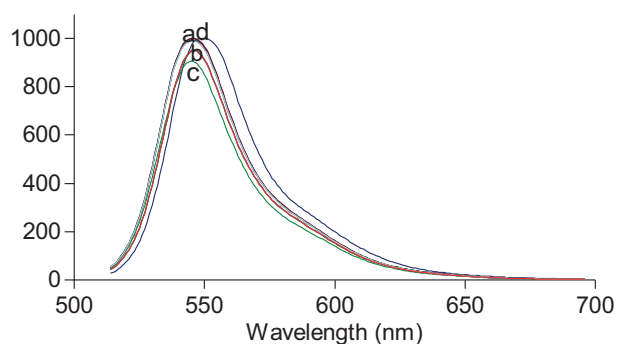


Figure 1. Emission spectra of eosin-Y dye in different moieties: a) emission of S2, S4, S5, S9 $\lambda_{\max}^{em} = 545$ nm; b) emission of S1, S7, S3; $\lambda_{\max}^{em} = 548$ nm; c) emission of S8; $\lambda_{\max}^{em} = 546$ nm; d) emission of S6; $\lambda_{\max}^{em} = 554$ nm.

solutions (S1–S6). S1 did not contain any additive while S2–S6 contained different additives, i.e. IL-I, IL-II, IL-III, SDS, and TX-100, respectively (Table 2). Figure 2 reveals the emission-based response of eosin-Y to the metal cations in additive-free S1 (Figure 2a) and surfactant-containing S5 (Figure 2b) and S6 (Figure 2c) acetic acid/acetate/EtOH solutions at pH 5.0. The response of eosin-Y to conventional anions was also investigated by exposure to the anion standard solution from Dionex. This solution contained ionic forms of $151 \text{ mg L}^{-1} \text{ SO}_4^{2-}$, $20.2 \text{ mg L}^{-1} \text{ F}^-$, $30.2 \text{ mg L}^{-1} \text{ Cl}^-$, $100 \text{ mg L}^{-1} \text{ NO}_2^-$, $100 \text{ mg L}^{-1} \text{ Br}^-$, $102 \text{ mg L}^{-1} \text{ NO}_3^-$, and $151 \text{ mg L}^{-1} \text{ PO}_4^{2-}$. Results are shown in Figure 3 in terms of relative signal changes, $((I - I_0)/I_0)$, where I is the fluorescence intensity of the dye after exposure to ion-containing solutions and I_0 is the fluorescence intensity of the dye in ion-free solutions. The emission intensity of eosin-Y was affected by most of the tested cations (Figure 2a) and anions (Figure 3) in additive-free solutions. However, presence of surfactants and/or ILs in the

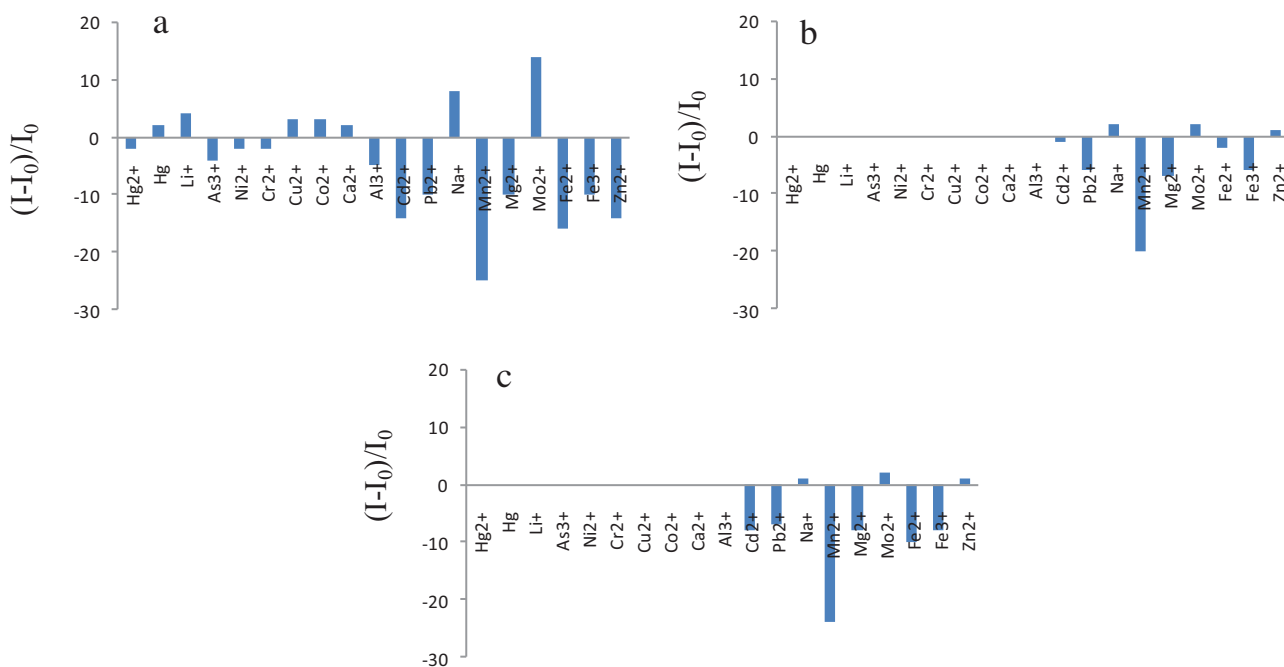


Figure 2. a) Response of eosin-Y to different cations in solutions of S1; b) Response of eosin-Y to different cations in solutions of S5; c) Response of eosin-Y to different cations in solutions of S6.

solutions completely suppressed the response of the dye towards interferent cations (see Figures 2b and 2c and Table 3). No response for the tested metal ions of Ca^{2+} , Cu^{2+} , Hg^{+} , Hg^{2+} , As^{5+} , Li^{+} , Al^{3+} , Cr^{3+} , Co^{2+} , or Ni^{2+} was observed in the tested solutions (S2–S6). The response to Na^{+} , Cd^{2+} , Zn^{2+} , and Mo^{2+} was suppressed to the level of 1% in both the IL- and surfactant-containing moieties. The analytical signal changes observed for the constituents of Pb^{2+} , Mg^{2+} , and Fe^{3+} were also significantly decreased.

Table 2. Compositions of the solutions.

Solution	Dye	Media	Additive conc. (M)
S1	10^{-5} M Eosin-Y	2.5 mL pH 5.0 buffer : EtOH mixture (60:40, v:v)	-
S2	10^{-5} M Eosin-Y	2.5 mL pH 5.0 buffer:EtOH mixture (60:40, v:v)	IL-I (2.14×10^{-2})
S3	10^{-5} M Eosin-Y	2.5 mL pH 5.0 buffer:EtOH mixture (60:40, v:v)	IL-II (2.61×10^{-2})
S4	10^{-5} M Eosin-Y	2.5 mL pH 5.0 buffer:EtOH mixture (60:40, v:v)	IL-III (2.17×10^{-2})
S5	10^{-5} M Eosin-Y	2.5 mL pH 5.0 buffer:EtOH mixture (60:40, v:v)	SDS (10^{-2})
S6	10^{-5} M Eosin-Y	2.5 mL pH 5.0 buffer:EtOH mixture (60:40, v:v)	TX-100 (2.0×10^{-3})
S7	10^{-5} M Eosin-Y	2.5 mL pH 5.0 buffer:IL-I mixture (60:40, v:v)	IL-I (2.14)
S8	10^{-5} M Eosin-Y	2.5 mL pH 5.0 buffer:IL-II mixture (60:40, v:v)	IL-II (2.61)
S9	10^{-5} M Eosin-Y	2.5 mL pH 5.0 buffer:IL-III mixture (60:40, v:v)	IL-III (2.17)

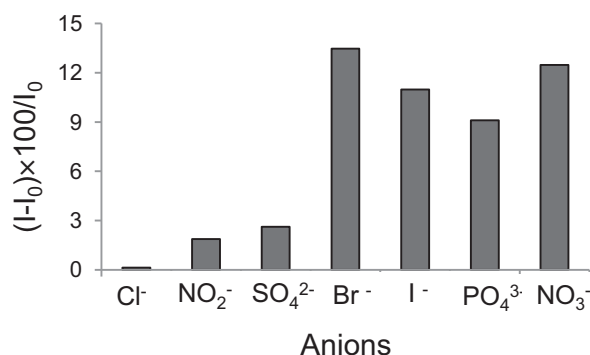


Figure 3. Response of eosin-Y to conventional anions in additive-free solution of S1.

The tolerance limits were also calculated for the most interfering species among the tested ions. The tolerance limit is an important parameter in interferent analysis and is expressed as the maximum interferent concentration in terms of mg L^{-1} that causes an error of 5% in the analytical signal. The results are shown in Table 3. From the results, it can be concluded that the cations Na^{+} and Zn^{2+} exhibited less interfering effect in IL- and micelle-containing media. The tolerance limits for Na^{+} and Zn^{2+} were enhanced 6-fold and 5.4-fold in the presence of $[\text{EMIM}][\text{BF}_4]$ and SDS, respectively.

Table 3. The tolerance limits (TL, mg L⁻¹) of the most interfering ions on the determination of 3.0 mg L⁻¹ Mn²⁺ in different tested solutions (S1–S6).

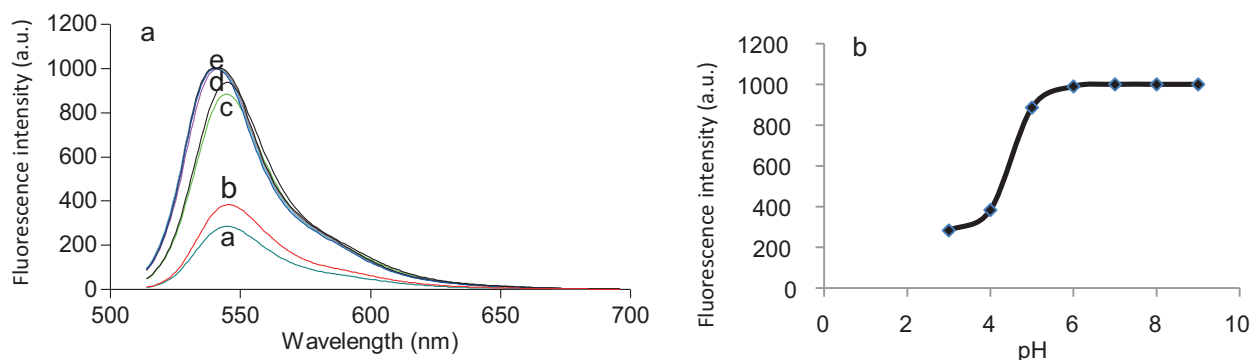
Interferent	TL in S1 (mg L ⁻¹)	TL in S2 (mg L ⁻¹)	TL in S3 (mg L ⁻¹)	TL in S4 (mg L ⁻¹)	TL in S5 (mg L ⁻¹)	TL in S6 (mg L ⁻¹)
Cd ²⁺	0.22	0.32	0.40	0.54	0.32	0.48
Pb ²⁺	0.40	0.40	0.22	0.28	0.40	0.22
Na ⁺	2.80	14.20	10.00	14.00	17.20	8.40
Mg ²⁺	0.22	0.42	0.40	0.42	0.40	0.48
Mo ²⁺	0.40	0.60	0.80	1.00	0.60	0.48
Fe ²⁺	0.40	0.28	0.28	0.32	0.48	0.54
Fe ³⁺	0.40	0.28	0.40	0.40	0.54	0.62
Zn ²⁺	3.20	16.20	5.40	17.40	13.80	4.60

2.3. Effect of pH on metal ion sensing ability of eosin-Y

The effect of pH on the emission spectra of eosin-Y was investigated in metal-free and Mn²⁺-containing buffered solutions. The solutions were prepared with a mixture of acetate buffer (0.01 M, pH 5.0) and EtOH (60:40; v:v). pH-induced emission-based response of eosin-Y is shown in Figure 4. The dye exhibited a decrease in signal intensity upon exposure to protons in the pH range of 3.0–9.0. The pKa value of the dye in the employed solution was calculated according to the following equation:

$$pKa = pH + \log[(I_x - I_b)/(I_a - I_x)], \quad (1)$$

where I_a and I_b are the fluorescence intensities of acidic and basic forms and I_x is the intensity at a pH near to the midpoint. The calculated pKa value is 4.79.

**Figure 4.** pH-induced emission spectra of 10⁻⁵ M eosin-Y after exposure to buffer solutions of (a) pH 3.0; (b) pH 4.0; (c) pH 5.0 (d); pH 6.0 (e); pH 7.0, 8.0, 9.0.

From Figure 4, it can be concluded that eosin-Y exhibits pH sensitivity around pH 4.76. Thus, pH of the working solutions should be kept constant with a high buffer capacity agent. In this work, we utilized 0.01 M acetic acid/acetate buffer to keep the pH constant at 5.0.

Effect of pH on determination of Mn²⁺ was investigated at fixed metal ion concentration in the pH range of 3.0–9.0 in all of the working solutions. Figure 5 shows the response of the dye to Mn²⁺ in additive-free solution S1. Eosin-Y exhibited the optimum analytical signal for Mn²⁺ at pH 5.0 in all of the studied solutions; therefore, pH 5.0 was chosen as the appropriate working condition for further studies. This result is consistent

with the literature stating that dye responses are best to the metal ion near its pKa value.³⁵ Table 4 shows the distribution of manganese species in aqueous environments taken from Minteq software. At working pH, all of the manganese species are in +2 forms in aqueous solutions.

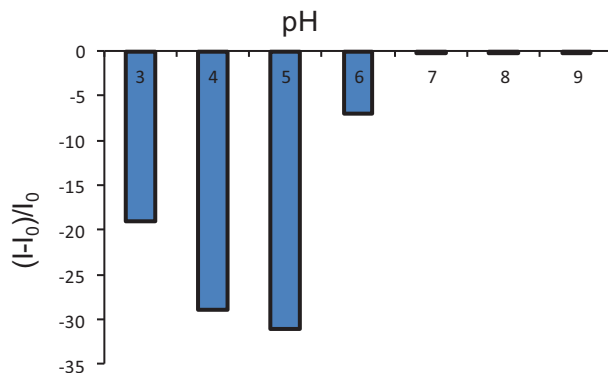


Figure 5. Response of eosin-Y to fixed amount of Mn²⁺ in buffered solutions between pH 3.0 and 9.0 ([Mn²⁺] = 1.0 mg L⁻¹).

Table 4. pH dependent distribution of manganese.

Component	Total dissolved (mol kg ⁻¹)	% dissolved
H ⁺	4.6822×10^{-6}	100.000
Mn ²⁺	1.0000	100.000

2.4. Response of eosin-Y to Mn²⁺

Eosin-Y exhibited a distinct quenching in fluorescence intensity at around 545 nm upon exposure to ionic manganese. According to the theory, fluorescence quenching can occur by two mechanisms: dynamic and static quenching. In the case of static quenching, the steady-state absorption spectrum of the chromophore is expected to be perturbed in the presence of a quencher that interacts and forms a complex with the chromophore in the ground state. In contrast, dynamic quenching does not cause any spectral change in the absorption spectra. For this reason, the nature of the ground state was investigated by studying the molecule's steady-state absorption spectrum. The absorption spectra of eosin-Y were recorded in a mixture of acetate buffer (0.01 M, pH 5.0) and EtOH (60:40; v:v) in the absence and presence of the quencher. Absorption spectra of the dye did not exhibit an appreciable change either in the absorption maxima or in the integral, in the presence of 1.5×10^{-5} M concentration of quencher. This observation eradicates the possibility of the formation of a ground state complex between the eosin-Y and Mn²⁺ and the quenching is of dynamic type. In this type of quenching, manganese ions efficiently quench the fluorescence of eosin-Y via collisions with the fluorophore in its excited state, leading to nonradiative energy transfer. The degree of quenching is related to the frequency of collisions, and therefore to the concentration, pressure, temperature, and matrix material of the sensing agent. Quenching-based response of eosin-Y to Mn²⁺ was recorded in different solutions,

S1–S9. The highest relative signal changes were obtained for S6 and S7. Figure 6 shows the response of eosin-Y to Mn²⁺ in S6 (Figure 6a) and S7 (Figure 6b). S6 and S7 contain 2×10^{-3} M TX-100 and 2.14 M IL-I, respectively. The insets of the figures show the calibration graphics of manganese, where concentration of the [Mn²⁺] was plotted versus relative signal intensity ((I - I₀)/I₀). Table 5 reveals the analytical response

parameters in all of the working solutions in terms of linear working range, calibration curve equation, limit of quantification (LOQ), LOD, and regression coefficient. The calibration curves were plotted by taking the mean values of three different solutions ($n = 3$) of the same medium. All of the exploited moieties exhibited a linear response to Mn^{2+} with considerably high slopes, which is evidence of high sensitivity. Among them, S6 exhibited the highest slope and R^2 value (see Table 5). The linear working ranges were $0.01\text{--}3.0\text{ mg L}^{-1}$ and $0.001\text{--}3.0\text{ mg L}^{-1}$ for S1–S6 and S7–S9, respectively. The IL-containing compositions S7–S9 exhibited larger linear working ranges with enhanced LOQ and LOD values with respect to the surfactant-containing moieties. The LOQ and LOD values were $1.0 \times 10^{-3}\text{ mg L}^{-1}$ and $2.5 \times 10^{-4}\text{ mg L}^{-1}$ for S7, which contained the optimum amount of IL-I. The LOD values were calculated by an equation using 3-fold the standard deviation of the mean value of 30 measurements of blank solutions. Presence of IL enhanced the limit of quantification 10-fold with respect to the IL-free solutions. The anionic form of eosin-Y makes an ion-pair with imidazolium cation and the analytical signal arises from the interaction of manganese with this species. Here, eosin-Y, which is a common fluorescent chelating agent, was used for the selective recognition of manganese. In this way, we obtained ten times better LOQ and higher selectivity with respect to the IL-free moieties.

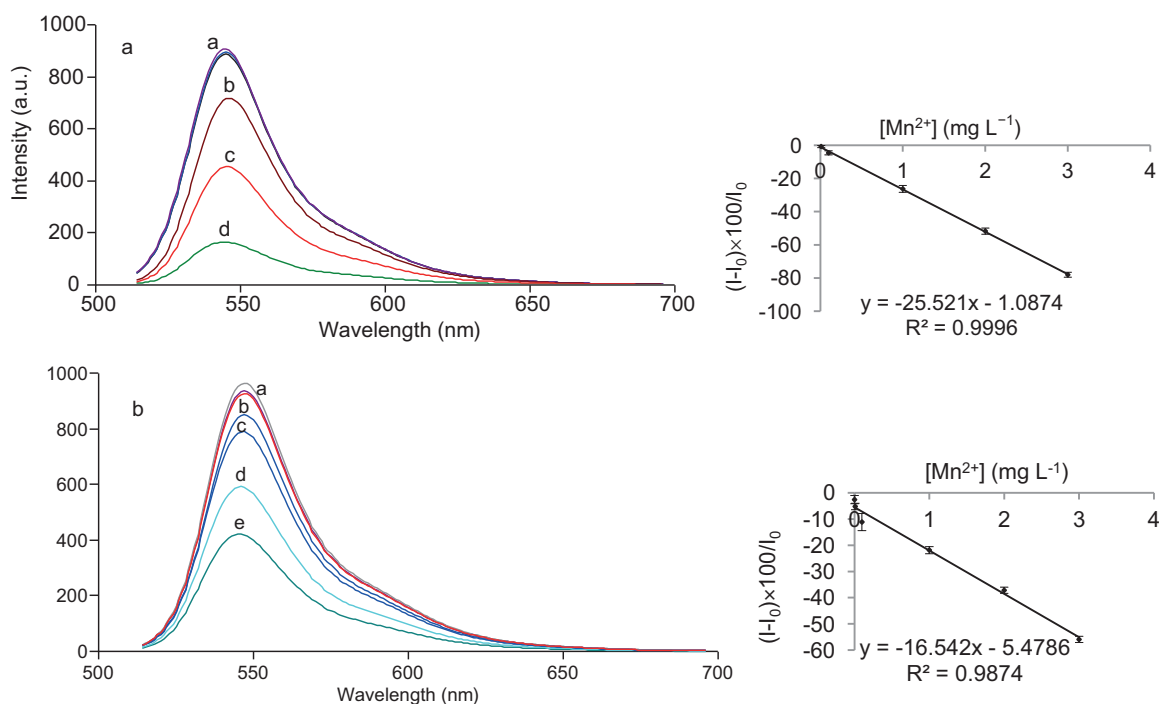


Figure 6. (a) Emission-based response of eosin-Y dye to Mn^{2+} in solution S6 in the concentration range of $0.0\text{--}3.0\text{ mg L}^{-1}$ Mn^{2+} : a) $0.0, 0.01, 0.1\text{ mg L}^{-1}$; b) 1.0 mg L^{-1} ; c) 2.0 mg L^{-1} ; d) 3.0 mg L^{-1} ; and Inset: emission-based calibration plot of eosin-Y in S6 for Mn^{2+} . (b) Emission-based response of eosin-Y dye to Mn^{2+} in solution S7 in the concentration range of $0.0\text{--}3.0\text{ mg L}^{-1}$ Mn^{2+} : a) $0.0, 0.001, 0.01\text{ mg L}^{-1}$; b) 0.1 mg L^{-1} ; c) 1.0 mg L^{-1} ; d) 2.0 mg L^{-1} ; e) 3.0 mg L^{-1} ; and Inset: emission-based calibration plot of eosin-Y for Mn^{2+} .

In higher concentrations of ILs ($>40\%$ by volume), no response to Mn^{2+} was seen. This can be attributed to probable quenching of eosin-Y with the IL because of the competing complex formation of the IL with the dye, which can interfere with the quenching response of eosin-Y with manganese. Mn^{2+} -induced relative signal changes for all test moieties are shown in Table 5. The best response was obtained for S6, where the presence of

TX-100 enhanced the relative signal change from 63% to 78%. The enhanced relative signal change of eosin-Y in the nonionic surfactant at concentrations higher than CMC can be attributed to micelle formation due to the interaction of the hydrophilic head group of Triton X-100 with the aqueous solution of hydrophilic eosin-Y. The arrangement of negatively charged eosin-Y molecules around the head group of Triton X-100 forms an attractive negative site for cationic manganese ions; thus an enhancement in the relative signal change of the dye was observed. Figure 7 shows the mechanism of micelle formation and the response of eosin-Y to manganese ions in the presence of Triton X-100. When the tests were performed in the anionic SDS, a slight decrease in the relative signal change was observed due to the repulsion and disorder between the carboxylate edge of eosin-Y and the head groups of the surfactant. Thus, we can conclude that noncharged micelles are better for the analysis of metal ions with respect to negatively charged reagents.

Table 5. Analytical characteristics of the response in different solutions.

Solution (mg L ⁻¹)	Linear working curve equation	Calibration (%)	RSC (mg L ⁻¹)	LOQ (mg L ⁻¹)	LOD (n = 3*)	R ²
S1	0.01–3.0	y = -21.584x - 2.4238	63	0.010	0.0030	0.9800
S2	0.01–3.0	y = -18.219x - 3.9658	61	0.010	0.0031	0.9875
S3	0.01–3.0	y = -19.739x - 0.8795	62	0.010	0.0026	0.9741
S4	0.01–3.0	y = -17.240x - 3.6874	58	0.010	0.0025	0.9893
S5	0.01–3.0	y = -19.519x - 5.5048	60	0.010	0.0028	0.9803
S6	0.01–3.0	y = -25.521x - 1.0874	78	0.010	0.0030	0.9996
S7	0.001–3.0	y = -16.542x - 5.4786	56	0.001	0.00025	0.9874
S8	0.001–3.0	y = -19.295x - 1.0141	60	0.001	0.00023	0.9969
S9	0.001–3.0	y = -17.764x - 5.2191	60	0.001	0.00035	0.9893

LOQ: Limit of quantification, LOD: Limit of detection, RSC: relative signal change,

R²: Regression coefficient

*The calibration curves were plotted by taking the mean values of three different solutions (n = 3) of the same media.

2.5. Determination of Mn²⁺ ions in real water samples

In order to verify the accuracy of the proposed method, recovery tests were performed for S6–S9. The proposed methods were applied for the determination of manganese in ultrapure and natural drinking water samples. The recovery tests were performed by spiking the water samples with different amounts of manganese before any pretreatment. For each water sample in the investigated media, three different solutions (n = 3) were prepared and analyzed. The recorded fluorescence intensities of the water samples were employed in the calibration equations. Solution of the calibration equations yielded the mean Mn²⁺ concentration of the water samples. Table 6 shows the obtained results. The recoveries were between 89.28% and 99.99%, confirming the accuracy of the method.

In the present study we employed three ILs (1-butyl-3-methylimidazolium thiocyanate ([BMIM][SCN]), 1-butyl-3-methylimidazolium tetrafluoroborate ([BMIM][BF₄]), and 1-ethyl-3-methylimidazolium tetrafluoroborate ([EMIM][BF₄]) and two micelles (sodium dodecyl sulfate (SDS) and Triton X-100) as new additives for the determination of Mn²⁺ with eosin-Y in aqueous solutions. The results revealed that the spectra of eosin-Y in all media exhibited a strong and selective fluorescence-based response to Mn²⁺. However, in the absence of the additives we observed emission-based cross-sensitivity for the metal ions Ca²⁺, Cu²⁺, Hg⁺, Hg²⁺, As⁵⁺, Li⁺, Al³⁺, Cr³⁺, Co²⁺, and Ni²⁺. Thus, the presence of ILs and surfactants suppressed the interfering effects

and significantly enhanced the selectivity of the dye to Mn^{2+} ions. The ILs also enhanced the LOD and the LOQ values 10-fold with respect to the IL-free moieties.

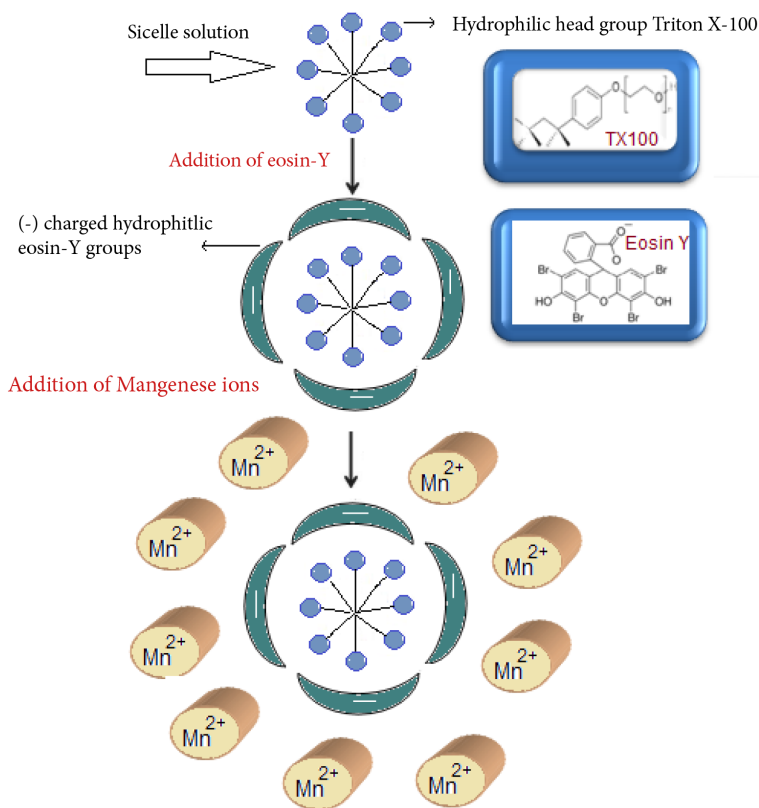


Figure 7. Response mechanism of eosin-Y to Mn^{2+} ions in the presence of Triton X-100.

Table 6. Determination of Mn^{2+} in real water samples.

Sample	Solution	Mn^{2+} added ($mg L^{-1}$)	Mn^{2+} found ($mg L^{-1}$) (n = 3, mean \pm SD)	Recovery (%)
Ultrapure water	S6	1.000	0.945 ± 0.016	94.17
	S7	1.000	0.953 ± 0.026	95.06
	S8	1.000	1.080 ± 0.036	92.59
	S9	1.000	0.925 ± 0.032	91.89
Drinking water	S6	0.010	$0.011 \pm 3.6 \times 10^{-3}$	90.90
		0.100	0.101 ± 0.072	99.99
		1.000	1.080 ± 0.036	92.59
		2.000	2.020 ± 0.104	99.00
	S7	0.010	0.011 ± 0.005	90.90
		0.100	0.112 ± 0.083	89.28
		1.000	1.082 ± 0.054	92.42
		2.000	1.959 ± 0.069	97.90

3. Experimental

3.1. Materials and methods

Stock solution of eosin-Y was prepared as 10^{-3} M in EtOH and diluted to 10^{-5} M during measurements. The determination of Mn^{2+} with eosin-Y was performed in the presence of the ILs 1-butyl-3-methylimidazolium tetrafluoroborate ([BMIM][BF₄]; IL-I), 1-ethyl-3-methylimidazolium tetrafluoroborate ([EMIM][BF₄]; IL-II) and 1-butyl-3-methylimidazolium thiocyanate [BMIM][SCN]; IL-III). Anionic and nonionic surfactants of sodium dodecyl sulfate (SDS) and Triton X-100 (TX-100) were used. Spectral analysis was performed at pH 5.0 in buffered solutions of H₂O:EtOH (60:40, v:v). Throughout the experiments 0.01 M acetic acid/acetate buffer solutions were used. Critical micelle concentrations of SDS and TX-100 were 10^{-3} M and 2.0×10^{-4} M, respectively. The micelle concentrations of the solutions were prepared to be 10-fold the CMC. Concentrations of the ILs were in the range of 2.14×10^{-2} – 2.61 M. The exact compositions of the utilized solutions are given in Table 2. The standard solutions of the metal ions were prepared by diluting certified reference standards of Merck for AAS (1000 mg L^{-1}) with Millipore ultrapure water. Absorption spectra were recorded using a Shimadzu 1601 UV-visible spectrophotometer. Steady-state fluorescence emission and excitation spectra were measured using a Varian Cary Eclipse Spectrofluorometer with a xenon flash lamp as the light source. pH measurements were recorded with an Orion pH meter.

Acknowledgments

Funding this research was provided by the Scientific Research Fund of Dokuz Eylül University (2012.KB.FEN.049 and 2009.KB.FEN.075) and TÜBİTAK (Kariyer Project 104M268).

References

1. Gerber, G. B.; Leonard, A.; Hantson, P. *Crit. Rev. Oncol. Hematol.* **2002**, *42*, 25-34.
2. Seleim, M. M.; Abu-Bakr, M. S.; Hashem, E. Y.; El-Zohry, A. M. *Can. J. Anal. Sci. Spect.* **2009**, *54*, 93-101.
3. Zatta, P.; Lucchini, R.; Rensburg, S. J.; Taylor, A. *Brain Res. Bull.* **2003**, *62*, 15-17.
4. Dias, F. D.; Alves, L. S.; Santos, W. N. L.; David, J. M.; Ferreira, S. L. C. *Anal. Lett.* **2009**, *42*, 2206-2213.
5. Almeida, L. F.; Vale, M. G. R.; Dessuy, M. B.; Silva, M. M.; Lima, R. S.; Santos, V. B.; Diniz P. H. D.; Araújo, M. C. U. *Talanta*. **2007**, *73*, 906-912.
6. Sreenivasa, Rao, K.; Balaji, T.; Prasada, Rao, T.; Babu, Y.; Naidu, G. R. K. *Spectrochim. Acta B.* **2002**, *57*, 1333-1338.
7. Weiss, H. V.; Kenis, P. R.; Korkisch, J.; Steffan, I. *Anal. Chim. Acta.* **1979**, *104*, 337-343.
8. Ruiz, M. C.; Rodriguez, M. H.; Perino, E.; Olsina, R. A. *Latin Am. Appl. Res.* **2004**, *34*, 23-27.
9. Beltagi, M.; Ismail, M. I.; Ghoneim, M. M. *Am. J. Anal. Chem.* **2013**, *4*, 197-206.
10. Ahrland, S.; Herman, R. G. *Anal. Chem.* **1975**, *47*, 2422-2426.
11. Shuhong, X.; Wang, C.; Zhang, H.; Sun, Q.; Wang, Z.; Cui, Y. J. *Mater. Chem.* **2012**, *22*, 9216-9221.
12. Liang, J.; Canary, J. W. *Angew. Chem. Int. Ed.* **2010**, *49*, 7710-7713.
13. Mao, X.; Su, H.; Tian, D.; Li, H.; Yang, R. *ACS Appl. Mater. Interfaces* **2013**, *5*, 592-597.
14. Gruppi, F.; Liang, J.; Bartelle, B.; Royzen, M.; Turnbull, D. H.; Canary, J. W. *Chem. Commun.* **2012**, *48*, 10778-10780.
15. <http://www.lifetechnologies.com/tr/en/home/references/molecular-probes-the-handbook/indicators-for-ca2-mg2-zn2-and-other-metal-ions.html>.

16. Bakthavatsalam S.; Sarkar, A.; Rakshit, A.; Jain, S.; Kumar, A.; Datta, A. *Chem. Commun. (Camb)*. **2015**, *51*, 2605-2608.
17. García, E. A.; Fernández, R. G.; Díaz-García, M. E. *Micropor. Mesopor. Mat.* **2005**, *77*, 235-239.
18. Oter, O.; Aydogdu, S. J. *Fluoresc.* **2011**, *21*, 43-50.
19. Merrigan, L.; Bates, E. D.; Dorman, S. C. *Chem. Commun.* **2000**, *20*, 2051-2052.
20. Öter, Ö.; Şahin, G. S. *Turk. J. Chem.* **2015**, *39*, 395-411.
21. Oter, O.; Sabanci, G.; Ertekin, K. *Sensor Letters* **2013**, *11*, 1-9.
22. Ongun, M. Z.; Oter, O.; Sabanci, G.; Ertekin, K.; Celik, E. *Sens. Actut. B-Chem.* **2013**, *183*, 11-19.
23. Matsumiya, H.; Kato, T.; Hiraide, M. *Talanta*. **2014**, *119*, 505-508.
24. Ríos, A. P.; Hernández-Fernández, F. J.; Lozano, L. J.; Sánchez-Segado, S.; Ginestá-Anzola, A., Godínez, C.; Tomás-Alonso, F.; Quesada, J. M. *J. Membr. Sci.* **2013**, *444*, 469-481.
25. Rios, A. P.; Hernandez-Fernandez, F. J.; Alguacil, F. J.; Lozano, L. J.; Ginesta, A.; Garcia-Diaz, I.; Sanchez-Segado, S.; Lopez, F. A.; Godinez, C. *Sep. Purif. Tech.* **2012**, *97*, 150-157.
26. Wellens, S.; Vander Hoogerstraete, T.; Möller, C.; Thijs, B.; Luyten, J.; Binnemans, K. *Hydrometallurgy* **2014**, *144*, 27-33.
27. Whitehead, J. A.; Zhang, J.; Pereira, N.; McCluskey, A.; Lawrance, G. A. *Hydrometallurgy* **2007**, *88*, 109-120.
28. Regel-Rosocka, M.; Nowak, L.; Wiśniewski, M. *Sep. Pur. Tech.* **2012**, *97*, 158-163.
29. Regel-Rosocka, M.; Wisniewski, M. *Hydrometallurgy* **2011**, *110*, 85-90.
30. Cheng, D. H.; Chen, X. W.; Shu, Y.; Wang, J. H. *Talanta* **2008**, *75*, 1270-1278.
31. Kogelniga, D.; Stojanovica, A.; Jirsa, F.; Kornerb, W.; Krachlera, R.; Kepplera, B. K. *Sep. Purif. Tech.* **2010**, *72*, 56-60.
32. Yanga, F.; Kubotaa, F.; Babaa, Y.; Kamiya, N.; Gotoa, M. *J. Hazard. Mater.* **2013**, *254-255*, 79-88.
33. Garcia, M. E. D.; Medel, A. S. *Talanta* **1986**, *33*, 255-264.
34. Safavi, A.; Abdollahi, H.; Maleki, N.; Zeinali, S. J. *Colloid Interf. Sci.* **2008**, *322*, 274-280.
35. Werner, T.; Wolfbeis, O. S. *Fresen. J. Anal. Chem.* **1993**, *346*, 564-568.
36. Dutta, K.; Deka, R.; Das, D. K. *J. Fluoresc.* **2013**, *23*, 1173-1178.
37. Seleim, M. M.; Abu-Bakr, M. S.; Hashem, E.Y.; El-Zohry, A. M. *Can. J. Anal. Sci. Spect.* **2009**, *54*, 93-101.
38. Kostova, D. J. *Anal. Chem.* **2010**, *65*, 159-163.
39. Ragos, G. C.; Demertzis, M. A.; Issopoulos, P. B. *Farmaco* **1997**, *52*, 199-203.
40. Tang, B.; Fang, H. *Anal. Lett.* **2001**, *34*, 1353-1368.